Journal of Solid State Chemistry 183 (2010) 1095–1101

Contents lists available at ScienceDirect

Journal of Solid State Chemistry

journal homepage: www.elsevier.com/locate/jssc

Structural and conductivity studies of $Y_{10-x}La_xW_2O_{21}$

Anna Lashtabeg [a,*], John Bradley [b], Andrew Dicks [b], Graeme Auchterlonie [a], John Drennan [a]

[a] ARC Centre of Excellence for Functional Nanomaterials, Australian Institute for Bioengineering and Nanotechnology (AIBN), University of Queensland, St Lucia, QLD 4072, Australia
[b] CSIRO National Hydrogen Materials Alliance, CSIRO Energy Centre, 10 Murray Dwyer Circuit, Steel River Estate, Mayfield West, NSW 2304, Australia

ARTICLE INFO

Article history:
Received 12 November 2009
Received in revised form
5 March 2010
Accepted 6 March 2010
Available online 18 March 2010

Keywords:
Structural characterisation
Lanthanum tungstate
Yttria tungstate
Conductivity studies

ABSTRACT

The aim of this work was to determine structural parameters of the $Y_{10-x}La_xW_2O_{21}$ ($x=0$–10) solid solution series and investigate their electric properties. Crystallographic data shows a gradual increase in symmetry with increasing La content, as the structure evolves from orthorhombic, $Y_{10}W_2O_{21}$, towards the pseudo-cubic structure of $Y_5La_5W_2O_{21}$. The solubility limit of La_2O_3 was found to be 50% ($x=5$). Above this level two phases were observed, $La_6W_2O_{15}$ and $(La,Y)_{10+x}W_{2-x}O_{21-\delta}$. The conductivity of Y rich samples was very low, with σ of the order 2×10^{-5}–$5\times10^{-5}\,S\,cm^{-1}$ at 1000 °C, whilst ionic conductivity was observed for most La rich doped samples. The highest conductivity was observed for $La_{10}W_2O_{21}$ and its doped analogues, at 1×10^{-3}–$5\times10^{-3}\,S\,cm^{-1}$ at 1000 °C. Unit cell parameters were determined as a function of temperature from 0 to 1000°C, and thermal expansion of these materials was determined from temperature studies carried out at the Australian Synchrotron facility in Melbourne, Victoria, Australia.

1. Introduction

There has been a wealth of studies on rare earth (RE) tungsten oxides in the system RE_2O_3–WO_3 [1–3] (RE=La–Lu and Y) as a result of the wide range of applications in which these materials can be employed, such as ferroelectrics, phosphors and refractory materials. Yttria tungstates have displayed a number of interesting properties, such as fluorescence [4] and negative thermal expansion [5] while lanthanum tungstates have been intensively studied as a result of some interesting electrochemical and optical properties: $La_xWO_{3+1.5x}$, ($x\cong6$) for example is known to exhibit proton conductivity in wet hydrogen at 900 °C [6–8].

Within the composition range RE_2O_3–RE_2WO_6 where the oxygen to metal ratio, O/M, is 1.5–2, these phases are generally examples of anion deficient, fluorite-related compounds with anion deficient superstructures. The phase diagram for the La_2O_3–WO_3 system has been investigated [9] and a large number of phases have been identified, of which the 5:2 phase ($La_{10}W_2O_{21}$) is one of the phases often confused with the high temperature 3:1 phase (La_6WO_{12}), which is a stoichiometry common to most of the other RE_2O_3–WO_3 and RE_2O_3–MoO_3 systems.

Although the 5:2 phase for lanthanum tungstate is thought to have a pyrochlore-related structure [9], there is little other information on its structure and no information on its electrochemical properties in the literature, thus little is known about the structure–properties relationship in this class of materials. In contrast, the phases $Ln_{10}W_2O_{21}$ occur unambiguously over a small compositional range in the smaller lanthanides for Ln=Nd–Er, Y [10], and are known to have orthorhombic unit cells based on a distorted fluorite parent structure.

The aim of this work was to determine structural parameters of the $Y_{10-x}La_xW_2O_{21}$ ($x=0$–10) solid solution series and investigate their electric properties. Other than structural information of $Y_{10}W_2O_{21}$ [10], no other information is available on this material. The electrochemical properties of $Y_{10}W_2O_{21}$ are examined and followed by doping this material with a dissimilar sized trivalent cation onto the Y site. In this paper La was chosen, and the structural and electrochemical properties were examined as a function of dopant concentration.

2. Experimental

Fluorite-related compounds in the $Y_{10-x}La_xW_2O_{21}$ series were prepared using a standard solid state reaction of dried metal oxides, Y_2O_3, La_2O_3 and WO_3 (Sigma Aldrich), with purities $>99.95\%$. The powders were mixed by hand in an agate mortar and pestle then pressed into pellets at 1.5 tonnes/cm^2. The pellets were buried in powder inside the Pt crucible and covered with an alumina lid in order to minimise WO_3 volatisation. The samples were reacted at 1350–1600 °C for up to 72 h with intermediate regrinding and re-pelletising, with heating and cooling ramp rates of 5 °C/min. The density of most samples was very low at 50–55%. Post-reaction sintering of pellets at 1600 °C for 8 h produced densities of 55–95% of theoretical density.

---

* Corresponding author.
E-mail address: a.lashtabeg@uq.edu.au (A. Lashtabeg).

0022-4596/$ - see front matter © 2010 Elsevier Inc. All rights reserved.
doi:10.1016/j.jssc.2010.03.009

Initial X-ray diffraction (XRD) was performed using a Bruker D8 Advance X-ray diffractometer with Cu$K\alpha$ radiation, with 2θ scanning range 5–90° at intervals of 0.01°, and with stepping time of 6 S. Silicon obtained from Gem Dugout (a=5.4301 Å ± 0.0001 Å—200 mesh) was used as a standard reference material.

Synchrotron X-ray diffraction data were collected at the Australian synchrotron facilities, equipped with a Si (1 1 1) monochromator. The samples were contained in 0.5 mm quartz capillaries, and data collected at 15 keV energy and 273–1273 K temperature range. Rietveld refinement and Pawley fitting were performed using Topas Academic V4.1 refinement software. The thermal expansion data were obtained from unit cell refinement of samples to 1273 K.

Transmission electron microscopy was performed on selected specimens. Samples were prepared by dispersing powders that had been crushed under dry ethanol on to copper grids coated with holey carbon film. The instrument used was a Jeol 2100 which was operated at an accelerating voltage of 200 keV.

Two-terminal AC impedance measurements were carried out in static air with a Solarton 1260 frequency response analyser, from 1 MHz to 0.1 Hz at an oscillation amplitude of 50 mV, with ZPlot/ZView software used for data collection and data analysis. Platinum paste was painted on each pellet face, fired at 900 °C for 1 h to form electrodes, and this process repeated until the resistance across the face of the pellet was less than 0.1 Ω. The samples were allowed for 1 h equilibration time after reaching each of the 50 measured temperatures before the measurement was initiated, with half of the measurements taken at regularly spaced intervals on the $1/T$ scale on the heating part of the cycle from room temperature up to 1000 °C, and the other half at intermediate temperatures on the cooling cycle. The data were modelled using ZView software and the errors for high resistance samples was in the range 0.1–0.01% due to the simplicity of the model using only one or two RC circuits. The bulk and the grain boundary responses for these high resistance samples were not distinguishable. The samples with lower resistances and ionic components were modelled using 2–3 RC circuits in parallel with the Warburg component. The errors on the fit were in the range 1–5% with increasing complexity of the model.

Thermo-gravimetric Analysis was carried out using Mettler-Toledo TGA/DSC1 module in flowing air at 20 ml/min, with heating and cooling ramp rates of 5 °C/min and 60 min dwell time at 1000 °C. The TGA instrument was calibrated using metal standards and the equipment baseline, measured with two empty crucibles, was subtracted.

3. Results and discussion

3.1. Crystal Structure

The newly measured unit cell of $Y_{10}W_2O_{21}$ is in good agreement with Bevan et al. [10], and formed a basis for the XRD refinement of doped samples up to x=0.25. $Y_{10}W_2O_{21}$ itself is described as a fluorite-related superlattice of 3 × 2 × 2 fluorite units with a=15.8761 Å, b=10.5232 Å and c=10.5778 Å, space group *Pbcn*, ICSD #35239 [10].

In the ideal fluorite structure the cations in eight-fold coordination with oxygen can be regarded as being in a chequerboard arrangement of cubes, with alternating occupied and empty polyhedra, and this arrangement of polyhedra is retained in the fluorite-related superlattice forming a three dimensional open structure (Fig. 1). In the $Y_{10}W_2O_{21}$ structure one in eight anions is absent with respect to fluorite and the cations have an average coordination number of seven, however the W cations are in sixfold coordination with O^{2-} in distorted octahedra while the Y cations are entirely sevenfold co-ordinate in one a/c layer, and equally seven and eight-fold co-ordinate in the successive a/c layer which they share with the tungsten (Fig. 1).

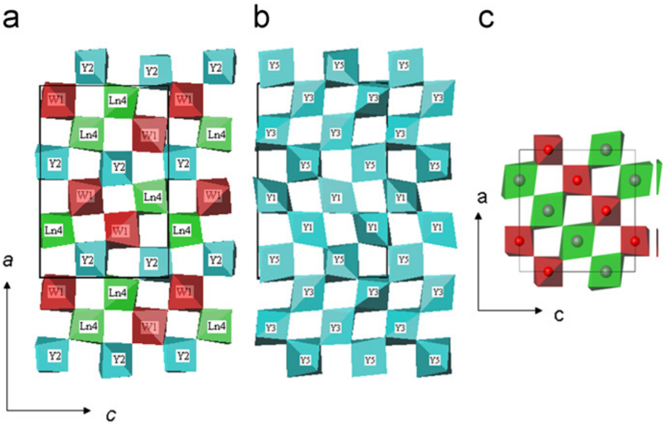

Fig. 1. (a) and (b) $Y_{10}W_2O_{21}$ viewed down the b axis, and showing two successive layers of cations at $y\sim0$ and $y\sim1/4$: blue 7 co-ordinate Y (Y1, Y2 and Y3), green 8 co-ordinate Y (Ln4), red 6 co-ordinate W (W1) (c) ideal cubic pyrochlore structure: red 6 co-ordinate cation, green 8 co-ordinate cation.

Analysis of the XRD data, Fig. 3, shows that the substitution of Y^{3+} by La^{3+} forms a solid solution series, $Y_{10-x}La_xW_2O_{21}$, with no additional lines corresponding to other phases up to the lanthanum rich phase x=7.5, whereupon the secondary orthorhombic phase $La_6W_2O_{15}$ forms and increases in concentration with further increase in yttria substitution, indicating La solubility in the Y sublattice up until at least x=5, i.e. 50% substitution. The materials in the stoichiometric range of x=0–2.5 crystallise in the parent orthorhombic unit cell and the XRD patterns in Fig. 3 show a shift in peak position consistent with increasing unit cell size as VII co-ordinated Y^{3+} (0.96 Å) is substituted by a larger VII co-ordinated La^{3+} cation (1.10 Å) (Table 1).

The *Ln*(4) site in$Y_{10}W_2O_{21}$ is the eight co-ordinate cation site [10], however the large distances between the *Ln*4 site and O(2) and O(5) sites, suggests that sixfold-triangular-prismatic coordination can also be considered reasonable for this cation. As a result of the larger size of La^{3+} in sevenfold coordination (1.10 Å) and eight-fold coordination (1.16 Å) compared to Y^{3+} (0.96 and 1.02 Å, respectively), it is apparent that the *Ln*4 site is an ideal La acceptor and preferential eight-fold coordination of La was assumed at the outset of the Rietveld refinements.

With increasing La^{3+} content the diffraction patterns show an increase in symmetry from orthorhombic $Y_{10}W_2O_{21}$, and at x=0.5, $Y_5La_5W_2O_{21}$, the cell can be indexed as face centred cubic, with a=10.873 (1) Å, a superlattice of 2 × 2 × 2 fluorite units similar to pyrochlore, $A_2B_2O_7$. Although $Y_5La_5W_2O_{21}$ may be indexed as face centred cubic from laboratory X-ray data the powder patterns show extra reflections that are systematic absences in the *Fd*-3*m* space group of pyrochlore. Synchrotron data show the asymmetry in the peak shape that is consistent with a smaller body-centred orthorhombic unit cell of a=7.6780 (4) Å, b=10.8596 (3) Å, c=7.6767 (3) Å, a superlattice of $\sqrt{2}\times2\times\sqrt{2}$, Fig. 2.

Indexing of the peaks for the synchrotron data strongly suggests $Y_5La_5W_2O_{21}$ belongs in the space group *Imm*2 (44), or one of the other three space groups indistinguishable by indexing in powder diffraction: *I*222 (23), $I2_12_12_1$ (24) and *Immm* (71). Initial attempts at Rietveld refinement of the synchrotron data in *Imm*2 shows that $Y_5La_5W_2O_{21}$ crystallises in a weberite type structure, $A'A''B'B''O_7$, which is very closely related to pyrochlore, however in weberite the A site cations occupy two slightly